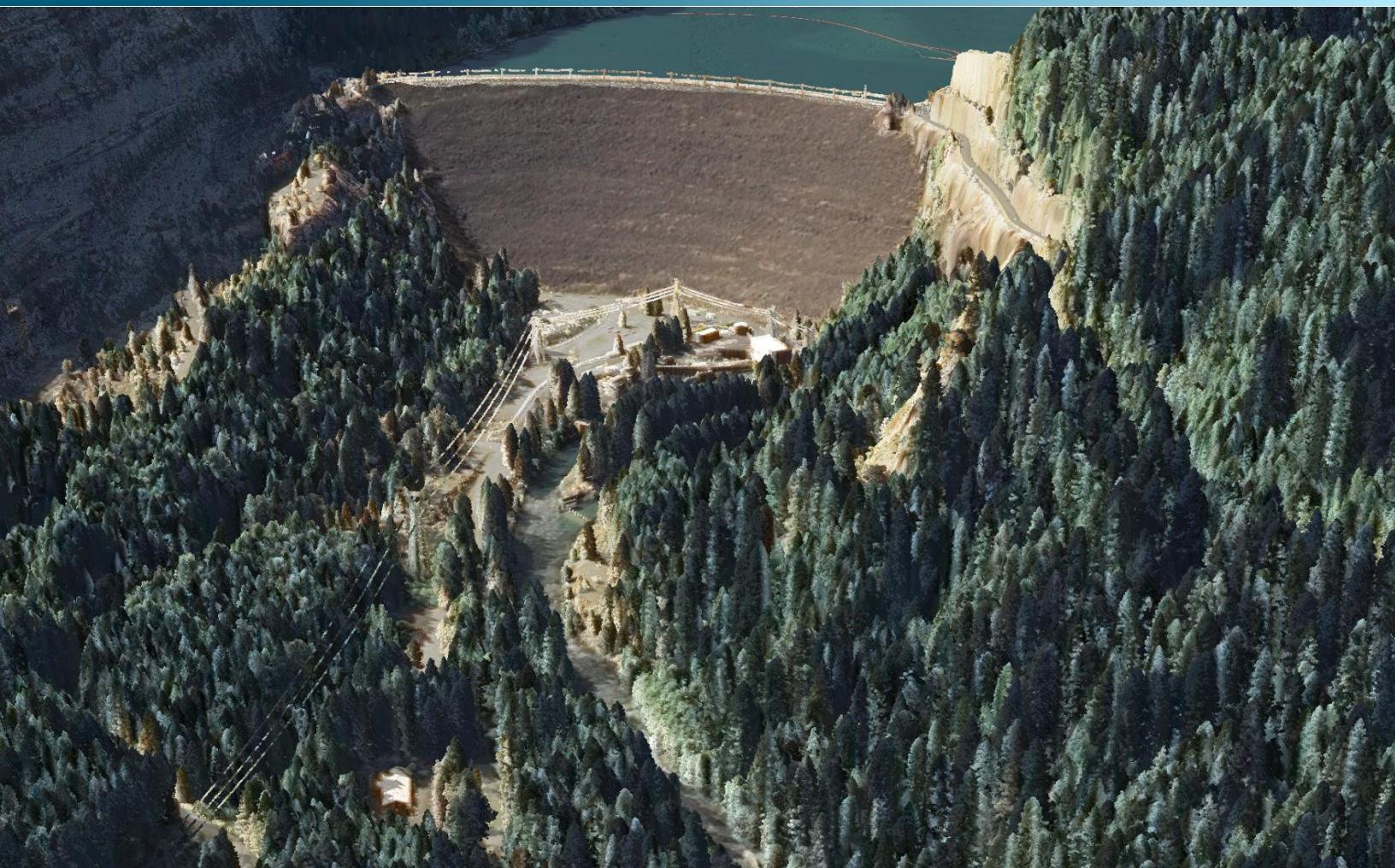


July 20, 2018



## McKenzie River, Oregon Topobathymetric LiDAR Technical Data Report

Prepared For:



**Mark Riley**

U.S. Forest Service Region 6  
1220 SW 3<sup>rd</sup> Ave.  
Portland, OR 97204  
PH: 503-808-2989

Prepared By:



**QSI Corvallis**

1100 NE Circle Blvd, Ste. 126  
Corvallis, OR 97330  
PH: 541-752-1204



## TABLE OF CONTENTS

INTRODUCTION .....	1
Deliverable Products .....	2
ACQUISITION .....	4
Sensor Selection: the Riegl VQ-880-G .....	4
Planning .....	4
Airborne Survey .....	6
LiDAR .....	6
Ground Control .....	7
Base Stations .....	7
Ground Survey Points (GSPs) .....	8
Land Cover Class .....	9
PROCESSING .....	11
Topobathymetric LiDAR Data .....	11
Bathymetric Refraction .....	14
LiDAR Derived Products .....	14
Topobathymetric DEMs .....	14
RESULTS & DISCUSSION .....	15
Bathymetric LiDAR .....	15
Mapped Bathymetry .....	15
LiDAR Point Density .....	16
First Return Point Density .....	16
Bathymetric and Ground Classified Point Densities .....	16
LiDAR Accuracy Assessments .....	20
LiDAR Non-Vegetated Vertical Accuracy .....	20
LiDAR Vegetated Vertical Accuracies .....	23
LiDAR Relative Vertical Accuracy .....	24
CERTIFICATIONS .....	26
SELECTED IMAGES .....	27
GLOSSARY .....	29
APPENDIX A - ACCURACY CONTROLS .....	30

**Cover Photo:** A view looking southwest at the termination of the South Fork of McKenzie River and Cougar Reservoir. The image was created from the LiDAR bare earth overlaid with the above ground point cloud and colored by orthoimagery.

## INTRODUCTION

This photo taken by QSI acquisition staff shows a view of GNSS Equipment set up over monument WC1413 to the north of McKenzie River priority areas 1 and 3.



In March 2018, Quantum Spatial (QSI) was contracted by U.S. Forest Service Region 6 (USFS) to collect topobathymetric Light Detection and Ranging (LiDAR) data in the spring of 2018 for the McKenzie River site in Oregon. The McKenzie River area of interest encompasses its southern fork as well as upstream reaches including Deer Creek and portions of the main stem to its intersection with Trail Bridge Reservoir. Traditional near-infrared (NIR) LiDAR was fully integrated with green wavelength return data (bathymetric) LiDAR in order to a comprehensive topobathymetric LiDAR dataset. Data were collected to aid USFS in assessing the channel morphology and topobathymetric surface of the study area to support river restoration and sediment manipulation activities of the McKenzie River and to acquire a greater understanding of fish habitat and vegetation structure within these reaches.

This report accompanies the delivered topobathymetric LiDAR data and documents contract specifications, data acquisition procedures, processing methods, and analysis of the final dataset including LiDAR accuracy, and density. Acquisition dates and acreage are shown in Table 1, a complete list of contracted deliverables provided to USFS is shown in Table 2, and the project extent is shown in Figure 1.

**Table 1: Acquisition dates, acreage, and data types collected on the McKenzie River site**

Project Site	Contracted Acres	Buffered Acres	Acquisition Dates	Data Type
McKenzie River, OR	3,056	3,638	04/26/2018	LiDAR

# Deliverable Products

**Table 2: Products delivered to USFS for the McKenzie River site**

<b>McKenzie River LiDAR Products</b>	
<b>Projection: Oregon Washington Albers</b>	
<b>Horizontal Datum: NAD83 (2011)</b>	
<b>Vertical Datum: NAVD88 (GEOID12B)</b>	
<b>Units: Meters</b>	
<b>Topobathymetric LiDAR</b>	
<b>Points</b>	<p>LAS v 1.4</p> <ul style="list-style-type: none"><li>• All Classified Returns</li></ul>
<b>Rasters</b>	<p>1.0 Meter ERDAS Imagine Files (*.img)</p> <ul style="list-style-type: none"><li>• Topobathymetric Bare Earth Digital Elevation Model (DEM) Bathymetric Voids Clipped</li><li>• Topobathymetric Bare Earth Digital Elevation Model (DEM) Bathymetric Voids Unclipped</li><li>• Highest Hit Digital Surface Model (DSM)</li></ul> <p>0.5 Meter ERDAS Imagine Files (*.img)</p> <ul style="list-style-type: none"><li>• Green Sensor Intensity Images</li><li>• NIR Sensor Intensity Images</li></ul>
<b>Vectors</b>	<p>Shapefiles (*.shp)</p> <ul style="list-style-type: none"><li>• Area of Interest</li><li>• LiDAR Tile Index</li><li>• Bathymetric Coverage Shape</li><li>• Water's Edge Breaklines</li><li>• Ground Survey Shapes</li><li>• Smooth Best Estimate Trajectory (SBETs)</li><li>• Flightline Swaths</li><li>• Flightline Index</li><li>• Total Area Flown</li></ul>

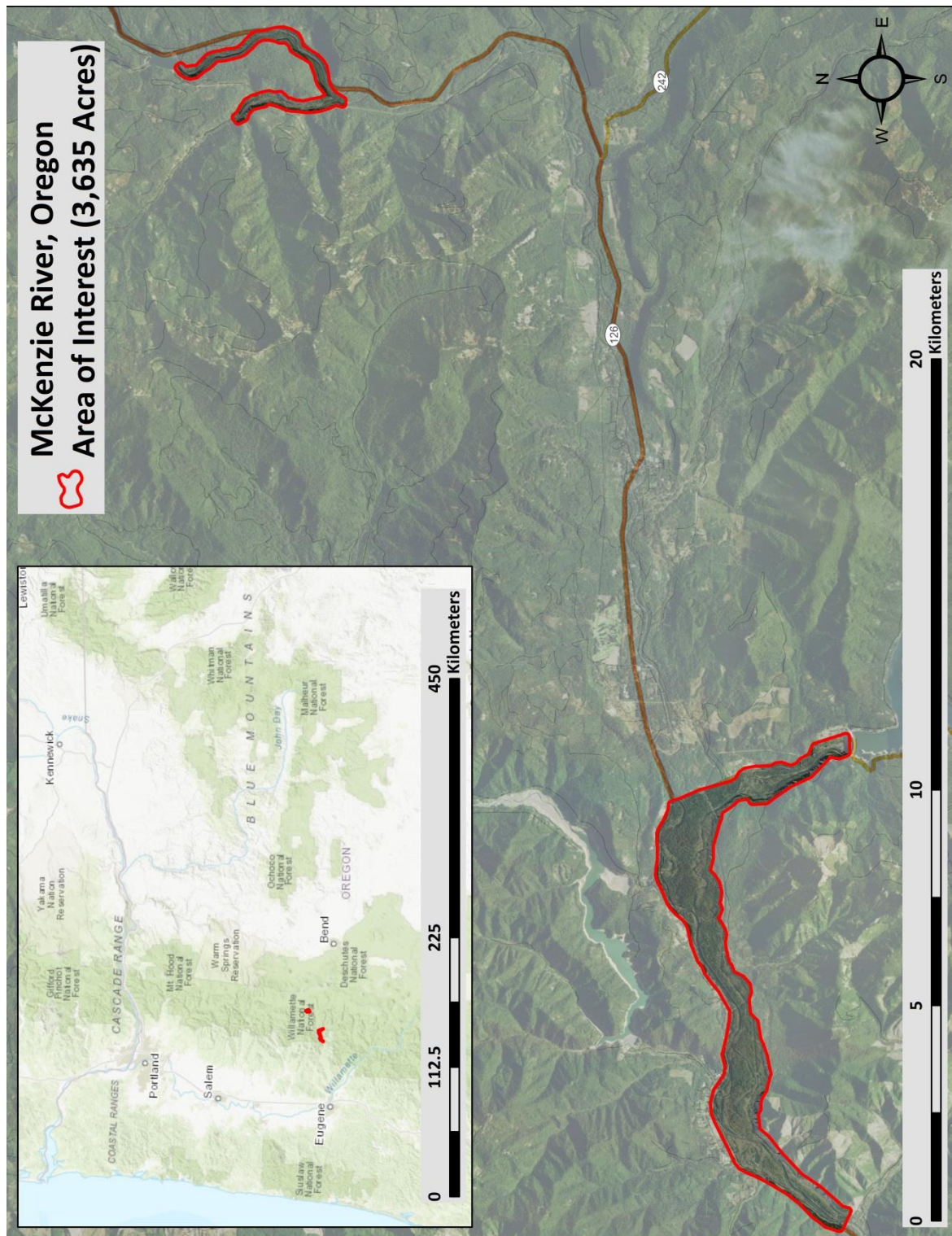


Figure 1: Location map of the McKenzie River site in Oregon

QSI's Cessna Caravan



### Sensor Selection: the Riegl VQ-880-G

The Riegl VQ-880-G was selected as the hydrographic airborne laser scanner for the McKenzie River project based on fulfillment of several considerations deemed necessary for effective mapping of the project site. A higher repetition pulse rate (up to 550 kHz), higher scanning speed, small laser footprint, and wide field of view allow for seamless collection of high resolution data of both topographic and bathymetric surfaces. A short laser pulse length allows for discrimination of underwater surface expression in shallow water, critical to shallow and dynamic environments such as the McKenzie River. Sensor specifications and settings for the McKenzie River acquisition are displayed in Table 3.

### Planning

In preparation for data collection, QSI reviewed the project area and developed a specialized flight plan to ensure complete coverage of the McKenzie River LiDAR study area at the target combined point density of  $\geq 8.0$  points/m<sup>2</sup> for Green and NIR LiDAR returns. Acquisition parameters including orientation relative to terrain, flight altitude, pulse rate, scan angle, and ground speed were adapted to optimize flight paths and flight times while meeting all contract specifications.

Factors such as satellite constellation availability and weather windows must be considered during the planning stage. Any weather hazards or conditions affecting the flight were continuously monitored due to their potential impact on the daily success of airborne and ground operations. In addition, logistical considerations including private property access, potential air space restrictions, channel flow rates (Figure 2 and Figure 3), and water clarity were reviewed.

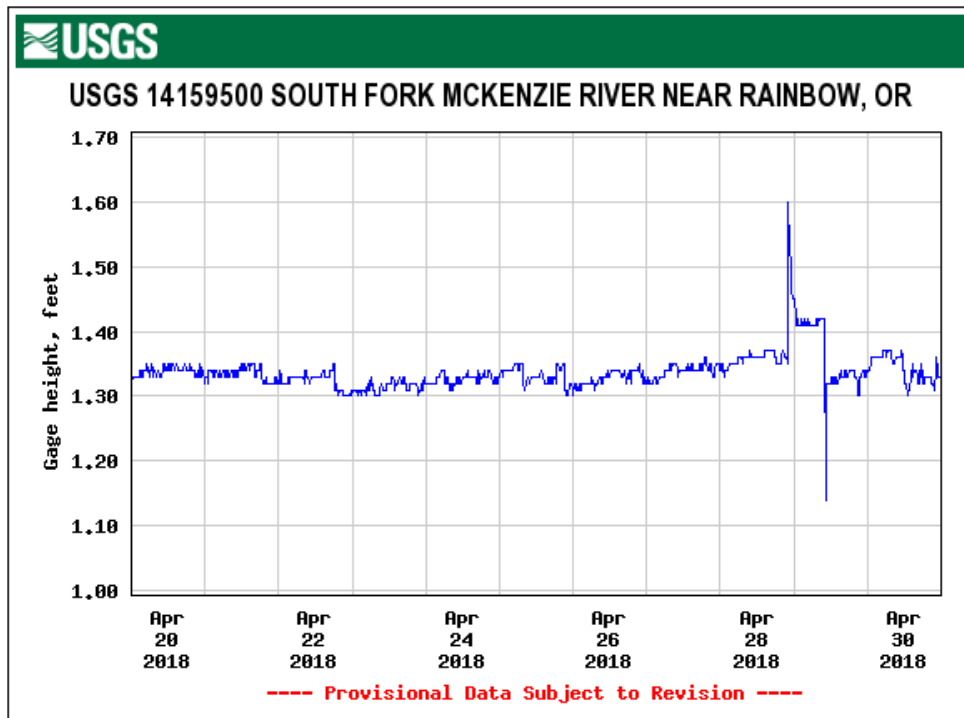


Figure 2: USGS Station 14159500 gauge height along the McKenzie River at the time of LiDAR acquisition.

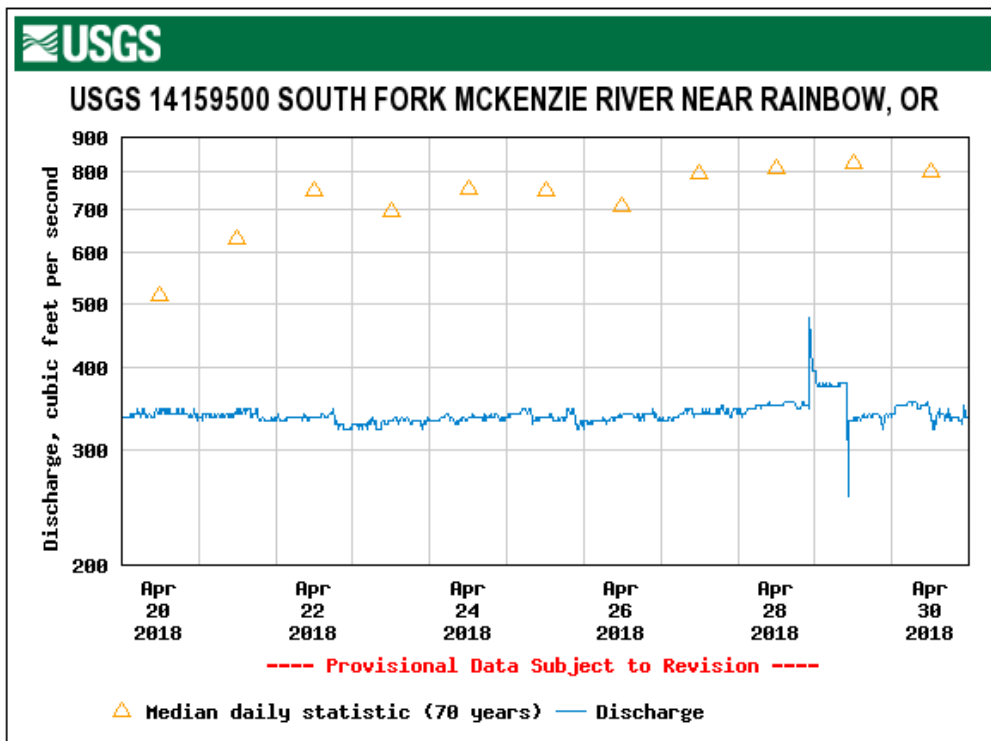


Figure 3: USGS Station 14159500 flow rates along the McKenzie River at the time of LiDAR acquisition.

# Airborne Survey

## LiDAR

The LiDAR survey was accomplished using a Riegl VQ-880-G green laser system mounted in a Cessna Caravan. The Riegl VQ-880-G uses a green wavelength ( $\lambda=532$  nm) laser that is capable of collecting high resolution vegetation and topography data, as well as penetrating the water surface with minimal spectral absorption by water. The Riegl VQ-880-G contains an integrated NIR laser ( $\lambda=1064$  nm) that adds additional topography data and aids in water surface modeling. The recorded waveform enables range measurements for all discernible targets for a given pulse. The typical number of returns digitized from a single pulse range from 1 to 7 for the McKenzie River project area. It is not uncommon for some types of surfaces (e.g., dense vegetation or water) to return fewer pulses to the LiDAR sensor than the laser originally emitted. The discrepancy between first return and overall delivered density will vary depending on terrain, land cover, and the prevalence of water bodies. All discernible laser returns were processed for the output dataset. Table 3 summarizes the settings used to yield an average pulse density of  $\geq 8$  pulses/m<sup>2</sup> over the McKenzie River project area.

**Table 3: LiDAR specifications and survey settings**

LiDAR Survey Settings & Specifications						
Acquisition Dates	April 26, 2018					
Aircraft Used	Cessna Caravan					
Priority Areas	1,3		2,6			
Sensor	Riegl					
Laser	VQ-880-G	VQ-880G-IR	VQ-880-G	VQ-880G-IR		
Maximum Returns	Unlimited					
Resolution/Density	Combined Average $\geq 8.0$ points/m <sup>2</sup>					
Nominal Pulse Spacing	0.35 m					
Survey Altitude (AGL)	750 m		900 m			
Survey speed	120 knots					
Field of View	40°					
Mirror Scan Rate	80 Lines Per Second	Uniform Point Spacing	80 Lines Per Second	Uniform Point Spacing		
Target Pulse Rate	245 kHz	145 kHz	245 kHz	145 kHz		
Pulse Length	1.5 ns	3 ns	1.5 ns	3 ns		
Pulse Width	45 cm	90 cm	45 cm	90 cm		
Central Wavelength	532 nm	1064 nm	532 nm	1064 nm		
Pulse Mode	Multiple Times Around (MTA)					
Beam Divergence	0.7 mrad	0.2 mrad	0.7 mrad	0.2 mrad		
Laser Pulse Footprint Diameter	52.5 cm	15 cm	63 cm	18 cm		
Swath Width	545.96 m		655.15 m			
Swath Overlap	63%					
Intensity	16-bit					
Accuracy NVA	$RMSE_z \leq 19.6$ cm					
Accuracy VVA	$RMSE_z \leq 29.4$ cm					

All areas were surveyed with an opposing flight line side-lap of  $\geq 50\%$  ( $\geq 100\%$  overlap) in order to reduce laser shadowing and increase surface laser painting. To accurately solve for laser point position (geographic coordinates x, y and z), the positional coordinates of the airborne sensor and the attitude of the aircraft were recorded continuously throughout the LiDAR data collection mission. Position of the aircraft was measured twice per second (2 Hz) by an onboard differential GPS unit, and aircraft attitude was measured 200 times per second (200 Hz) as pitch, roll and yaw (heading) from an onboard inertial measurement unit (IMU). To allow for post-processing correction and calibration, aircraft and sensor position and attitude data are indexed by GPS time.

## Ground Control

Ground control surveys, including monumentation and ground survey points (GSPs), were conducted to support the airborne acquisition. Ground control data were used to geospatially correct the aircraft positional coordinate data and to perform quality assurance checks on final LiDAR data.



USACE Monument WC1413

## Base Stations

Base stations were used for collection of ground survey points using real time kinematic (RTK) survey techniques. Base station locations were selected with consideration for satellite visibility, field crew safety, and optimal location for GSP coverage. QSI utilized one existing monument and two permanent base stations from the Leica Smartnet GNSS Network for the McKenzie River LiDAR project (Table 4, Figure 4). QSI's professional land surveyor, Evon Silvia (ORPLS#81104) oversaw and certified the ground survey.

**Table 4: Base station locations for the McKenzie River acquisition.**  
Coordinates are on the NAD83 (2011) datum, epoch 2010.00

PID	Latitude	Longitude	Ellipsoid (meters)	Type
OROR	43° 44' 46.95357"	-122° 29' 06.91043"	327.722	Leica Smartnet Station
ORSH	44° 23' 51.55697"	-122° 43' 39.26386"	150.562	Leica Smartnet Station
WC1413	44° 10' 26.56486"	-122° 17' 02.44009"	393.091	USACE Monument

QSI collected multiple static Global Navigation Satellite System (GNSS) occupations (1 Hz recording frequency) for the base station locations. During post-processing, the static GNSS data were triangulated with nearby Continuously Operating Reference Stations (CORS) using the Online Positioning User Service (OPUS) for precise positioning to ensure alignment with the National Spatial Reference System (NSRS). Multiple independent sessions for each position were processed to confirm antenna height measurements and to refine position accuracy.

## Ground Survey Points (GSPs)

Ground survey points were collected using real time kinematic (RTK) survey techniques. A QSI base station or the Leica Smartnet RTN broadcasted kinematic corrections to a roving Trimble R6 GNSS receiver. All GSP measurements were made during periods with a Position Dilution of Precision (PDOP) of  $\leq 3.0$  with at least six satellites in view of the stationary and roving receivers. When collecting RTK data, the rover records data while stationary for five seconds, then calculates the pseudorange position using at least three one-second epochs. Relative errors for any GSP position must be less than 1.5 cm horizontal and 2.0 cm vertical in order to be accepted. See Table 5 for Trimble unit specifications.

GSPs were collected in areas where good satellite visibility was achieved on paved roads and other hard surfaces such as gravel or packed dirt roads. GSP measurements were not taken on highly reflective surfaces such as center line stripes or lane markings on roads due to the increased noise seen in the laser returns over these surfaces. GSPs were collected within as many flightlines as possible; however the distribution of GSPs depended on ground access constraints and monument locations and may not be equitably distributed throughout the study area (Figure 4).

**Table 5: Trimble equipment identification**

Receiver Model	Antenna	OPUS Antenna ID	Use
Trimble R7	Zephyr GNSS Geodetic Model 2 RoHS	TRM57971.00	Static
Trimble R6	Integrated GNSS Antenna R6	TRM_R6	Rover

## Land Cover Class

In addition to ground survey points, land cover class check points were collected throughout the study area to evaluate vertical accuracy. Vertical accuracy statistics were calculated for all land cover types to assess confidence in the LiDAR derived ground models across land cover classes (Table 6, see LiDAR Accuracy Assessments, page 19).

**Table 6: Land Cover Types and Descriptions**

Land cover type	Land cover code	Example	Description	Accuracy Assessment Type
Tall Grass	TALL_GRASS (TG)		Herbaceous grasslands in advanced stages of growth	VVA
Forest	DEC_FOR (FR)		Forested areas dominated by deciduous species	VVA
Shrub	SHRUB (SH)		Areas dominated by lowland brush and woody vegetation less than 6m tall	VVA
Bare Earth	BARE (BE)		Areas of bare earth surface	NVA
Urban	URBAN (UA)		Areas dominated by urban development, including parks	NVA

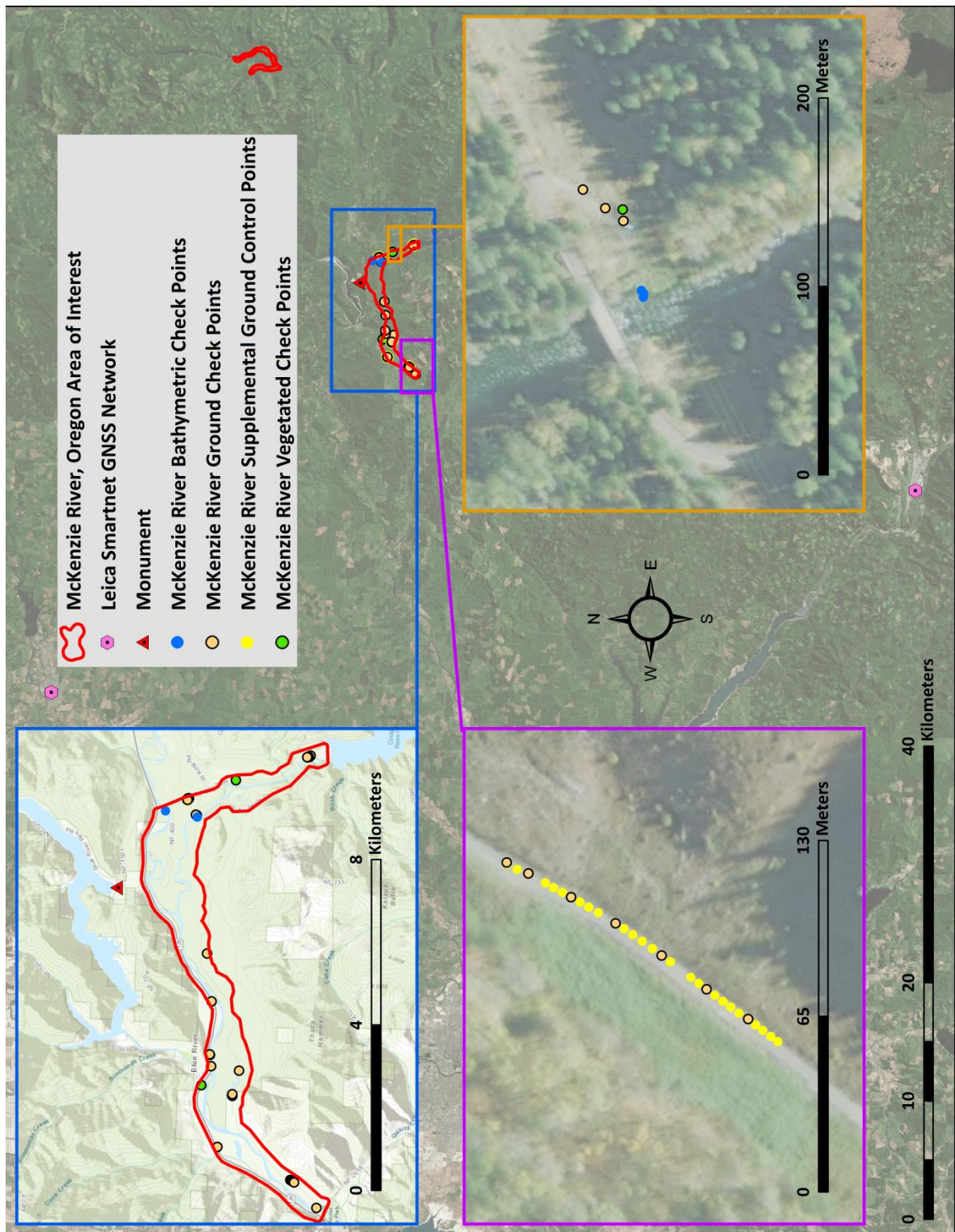
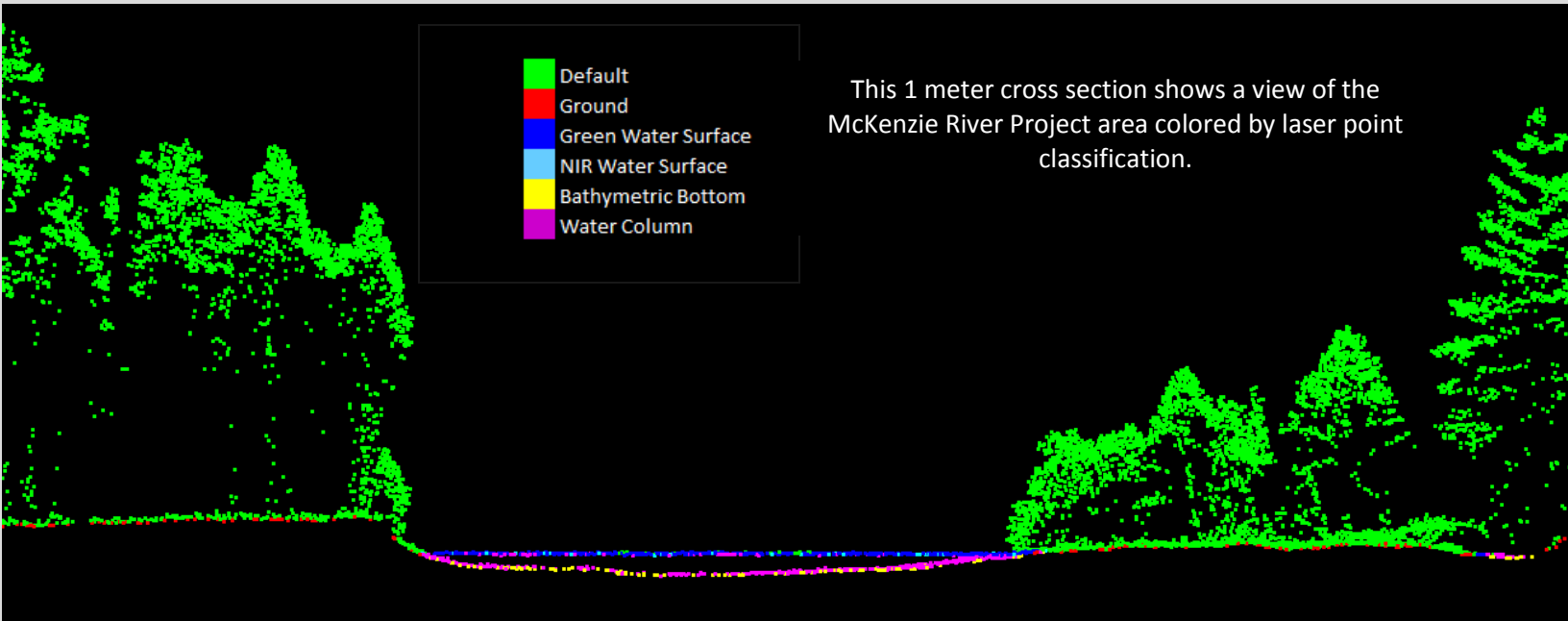


Figure 4: Ground Survey Location Map

## PROCESSING



This 1 meter cross section shows a view of the McKenzie River Project area colored by laser point classification.

### Topobathymetric LiDAR Data

Upon completion of data acquisition, QSI processing staff initiated a suite of automated and manual techniques to process the data into the requested deliverables. Processing tasks included GPS control computations, smoothed best estimate trajectory (SBET) calculations, kinematic corrections, calculation of laser point position, sensor and data calibration for optimal relative and absolute accuracy, and LiDAR point classification (Table 7).

Riegl's RiProcess software was used to facilitate bathymetric return processing. Once bathymetric points were differentiated, they were spatially corrected for refraction through the water column based on the angle of incidence of the laser. QSI refracted water column points using QSI's proprietary LAS processing software, Las Monkey. The resulting point cloud data were classified using both manual and automated techniques. Processing methodologies were tailored for the landscape. Brief descriptions of these tasks are shown in Table 8.

**Table 7: ASPRS LAS classification standards applied to the McKenzie River dataset**

Classification Number	Classification Name	Classification Description
1	Default/Unclassified	Laser returns that are not included in the ground class, composed of vegetation and anthropogenic features
10	Default/Unclassified Overlap	Flightline edge clip
2	Ground	Laser returns that are determined to be ground using automated and manual cleaning algorithms
7	Noise	Laser returns that are often associated with birds, scattering from reflective surfaces, or artificial points below the ground surface
9	Water	NIR Laser returns that are determined to be water using automated and manual cleaning algorithms
45	Water Column	Refracted Riegl sensor returns that are determined to be water using automated and manual cleaning algorithms.
40	Bathymetric Bottom	Refracted Riegl sensor returns that fall within the water's edge breakline which characterize the submerged topography.
41	Water Surface	Green laser returns that are determined to be water surface points using automated and manual cleaning algorithms.

**Table 8: LiDAR processing workflow**

LiDAR Processing Step	Software Used
Resolve kinematic corrections for aircraft position data using kinematic aircraft GPS and static ground GPS data. Develop a smoothed best estimate of trajectory (SBET) file that blends post-processed aircraft position with sensor head position and attitude recorded throughout the survey.	POSPac MMS v.8.2
Calculate laser point position by associating SBET position to each laser point return time, scan angle, intensity, etc. Create raw laser point cloud data for the entire survey in *.las (ASPRS v. 1.4) format. Convert data to orthometric elevations by applying a geoid correction.	RiProcess v1.8.5 TerraMatch v.18
Import raw laser points into manageable blocks to perform manual relative accuracy calibration and filter erroneous points. Classify ground points for individual flight lines.	TerraScan v.18
Using ground classified points per each flight line, test the relative accuracy. Perform automated line-to-line calibrations for system attitude parameters (pitch, roll, heading), mirror flex (scale) and GPS/IMU drift. Calculate calibrations on ground classified points from paired flight lines and apply results to all points in a flight line. Use every flight line for relative accuracy calibration.	TerraMatch v.18
Apply refraction correction to all subsurface returns.	Las Monkey 2.3 (QSI proprietary)
Classify resulting data to ground and other client designated ASPRS classifications (Table 7). Assess statistical absolute accuracy via direct comparisons of ground classified points to ground control survey data.	TerraScan v.18 TerraModeler v.18
Generate bare earth models as triangulated surfaces. Generate highest hit models as a surface expression of all classified points. Export all surface models in ERDAS Imagine (.img) format at a 1 meter pixel resolution.	TerraScan v.18 TerraModeler v.18 ArcMap v. 10.3.1
Export intensity images as GeoTIFFs at a 0.5 meter pixel resolution.	TerraScan v.18 TerraModeler v.18 ArcMap v. 10.3.1

## Bathymetric Refraction

The water surface model used for refraction is generated using NIR points within the breaklines defining the water's edge. Points are filtered and edited to obtain the most accurate representation of the water surface and are used to create a water surface model TIN. A tin model is preferable to a raster based water surface model to obtain the most accurate angle of incidence during refraction. The refraction processing is done using Las Monkey; QSI's proprietary LiDAR processing tool. After refraction, the points are compared against bathymetric control points to assess accuracy.

## LiDAR Derived Products

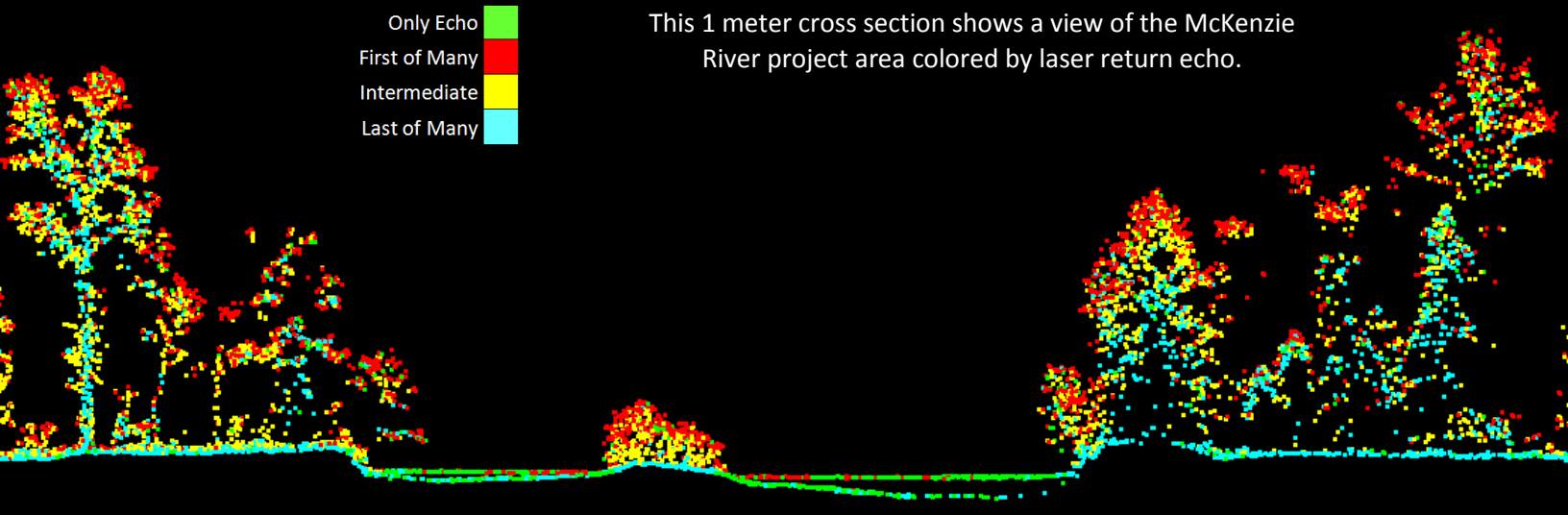
Because hydrographic laser scanners penetrate the water surface to map submerged topography, this affects how the data should be processed and presented in derived products from the LiDAR point cloud. The following discusses certain derived products that vary from the traditional (NIR) specification and delivery format.

### Topobathymetric DEMs

Bathymetric bottom returns can be limited by depth, water clarity, and bottom surface reflectivity. Water clarity and turbidity affects the depth penetration capability of the green wavelength laser with returning laser energy diminishing by scattering throughout the water column. Additionally, the bottom surface must be reflective enough to return remaining laser energy back to the sensor at a detectable level. Although the predicted depth penetration range of the Riegl VQ-880-G sensor is 1.5 Secchi depths on brightly reflective surfaces, it is not unexpected to have no bathymetric bottom returns in turbid or non-reflective areas.

As a result, creating digital elevation models (DEMs) presents a challenge with respect to interpolation of areas with no returns. Traditional DEMs are “unclipped”, meaning areas lacking ground returns are interpolated from neighboring ground returns (or breaklines in the case of hydro-flattening), with the assumption that the interpolation is close to reality. In bathymetric modeling, these assumptions are prone to error because a lack of bathymetric returns can indicate a change in elevation that the laser can no longer map due to increased depths. The resulting void areas may suggest greater depths, rather than similar elevations from neighboring bathymetric bottom returns. Therefore, QSI created a water polygon with bathymetric coverage to delineate areas with successfully mapped bathymetry. This shapefile was used to control the extent of the delivered clipped topobathymetric model to avoid false triangulation (interpolation from TIN'ing) across areas in the water with no bathymetric returns.

## RESULTS & DISCUSSION



### Bathymetric LiDAR

An underlying principle for collecting hydrographic LiDAR data is to survey near-shore areas that can be difficult to collect with other methods, such as multi-beam sonar, particularly over large areas. In order to determine the capability and effectiveness of the bathymetric LiDAR, QSI considered bathymetric return density and spatial accuracy.

### Mapped Bathymetry

The specified depth penetration range of the Riegl VQ-880-G sensor is 1.5 secchi depths; therefore, bathymetry data below 1.5 secchi depths at the time of acquisition is not to be expected. To assist in evaluating performance results of the sensor, a polygon layer was created to delineate areas where bathymetry was successfully mapped.

This shapefile was used to control the extent of the delivered clipped topo-bathymetric model and to avoid false triangulation across areas in the water with no returns. Insufficiently mapped areas were identified by triangulating bathymetric bottom points with an edge length maximum of 4.56 meters. This ensured all areas of no returns ( $> 9 \text{ m}^2$ ), were identified as data voids. Overall, QSI mapped 82.8% of the bathymetry within the McKenzie River project area.

# LiDAR Point Density

## First Return Point Density

The acquisition parameters were designed to acquire an average first-return density of 8 points/m<sup>2</sup>. First return density describes the density of pulses emitted from the laser that return at least one echo to the system. Multiple returns from a single pulse were not considered in first return density analysis. Some types of surfaces (e.g., breaks in terrain, water and steep slopes) may have returned fewer pulses than originally emitted by the laser.

First returns typically reflect off the highest feature on the landscape within the footprint of the pulse. In forested or urban areas the highest feature could be a tree, building or power line, while in areas of unobstructed ground, the first return will be the only echo and represents the bare earth surface.

The average first-return density of the McKenzie River LiDAR project was 29.87 points/m<sup>2</sup> (Table 9). The statistical and spatial distributions of all first return densities per 100 m x 100 m cell are portrayed in Figure 5 and Figure 7.

## Bathymetric and Ground Classified Point Densities

The density of ground classified LiDAR returns and bathymetric bottom returns were also analyzed for this project. Terrain character, land cover, and ground surface reflectivity all influenced the density of ground surface returns. In vegetated areas, fewer pulses may have penetrated the canopy, resulting in lower ground density. Similarly, the density of bathymetric bottom returns was influenced by turbidity, depth, and bottom surface reflectivity. In turbid areas, fewer pulses may have penetrated the water surface, resulting in lower bathymetric density.

The ground and bathymetric bottom classified density of LiDAR data for the McKenzie River project was 2.09 points/m<sup>2</sup> (Table 9). The statistical and spatial distributions ground classified and bathymetric bottom return densities per 100 m x 100 m cell are portrayed in Figure 6 and Figure 8.

Additionally, for the McKenzie River project, density values of only bathymetric bottom returns were calculated for areas containing at least one bathymetric bottom return. Areas lacking bathymetric returns (voids) were not considered in calculating an average density value. Within the successfully mapped area, a bathymetric bottom return density of 2.08 points/m<sup>2</sup> was achieved.

**Table 9: Average LiDAR point densities**

Density Type	Point Density
Green Laser First Returns	29.87 points/m <sup>2</sup>
Ground and Bathymetric Bottom Classified Returns	2.09 points/m <sup>2</sup>
Bathymetric Bottom Classified Returns	2.08 points/m <sup>2</sup>

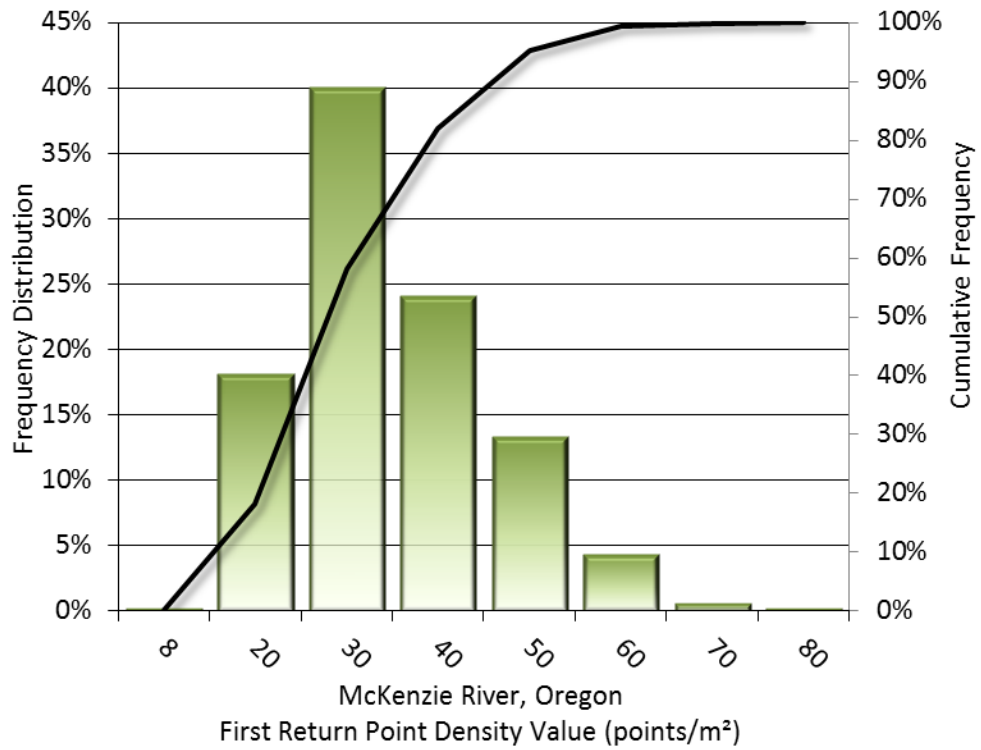


Figure 5: Frequency distribution of first return densities per 100 x 100 m cell

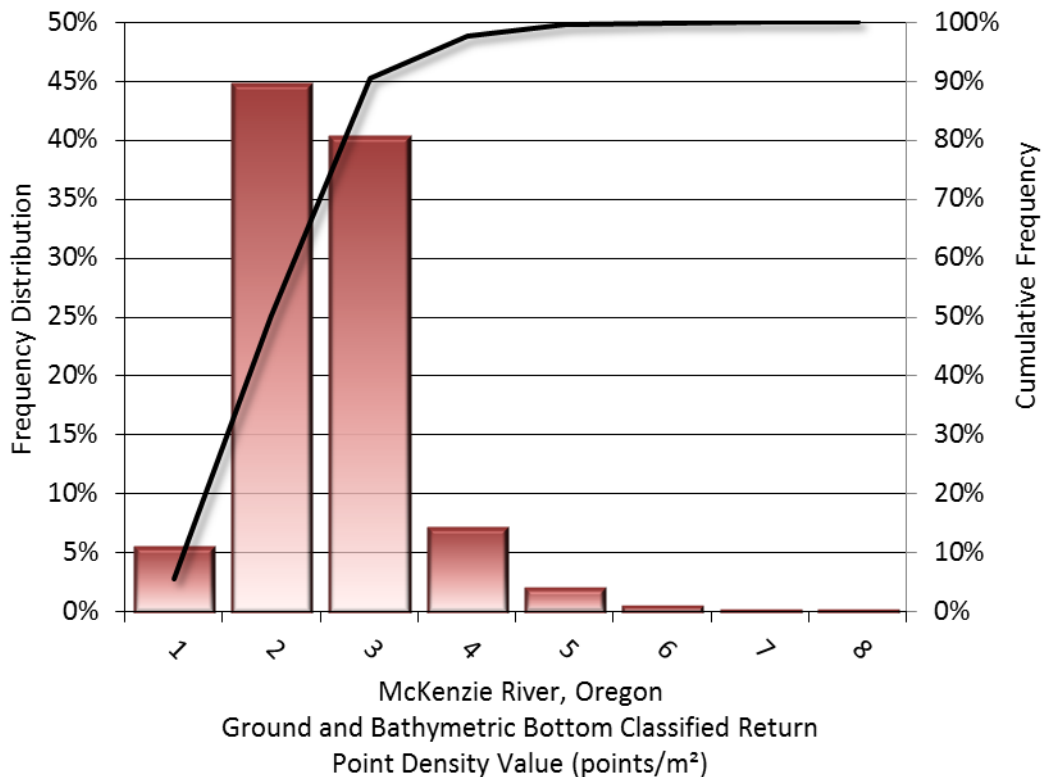


Figure 6: Frequency distribution of ground and bathymetric bottom classified return densities per 100 x 100 m cell

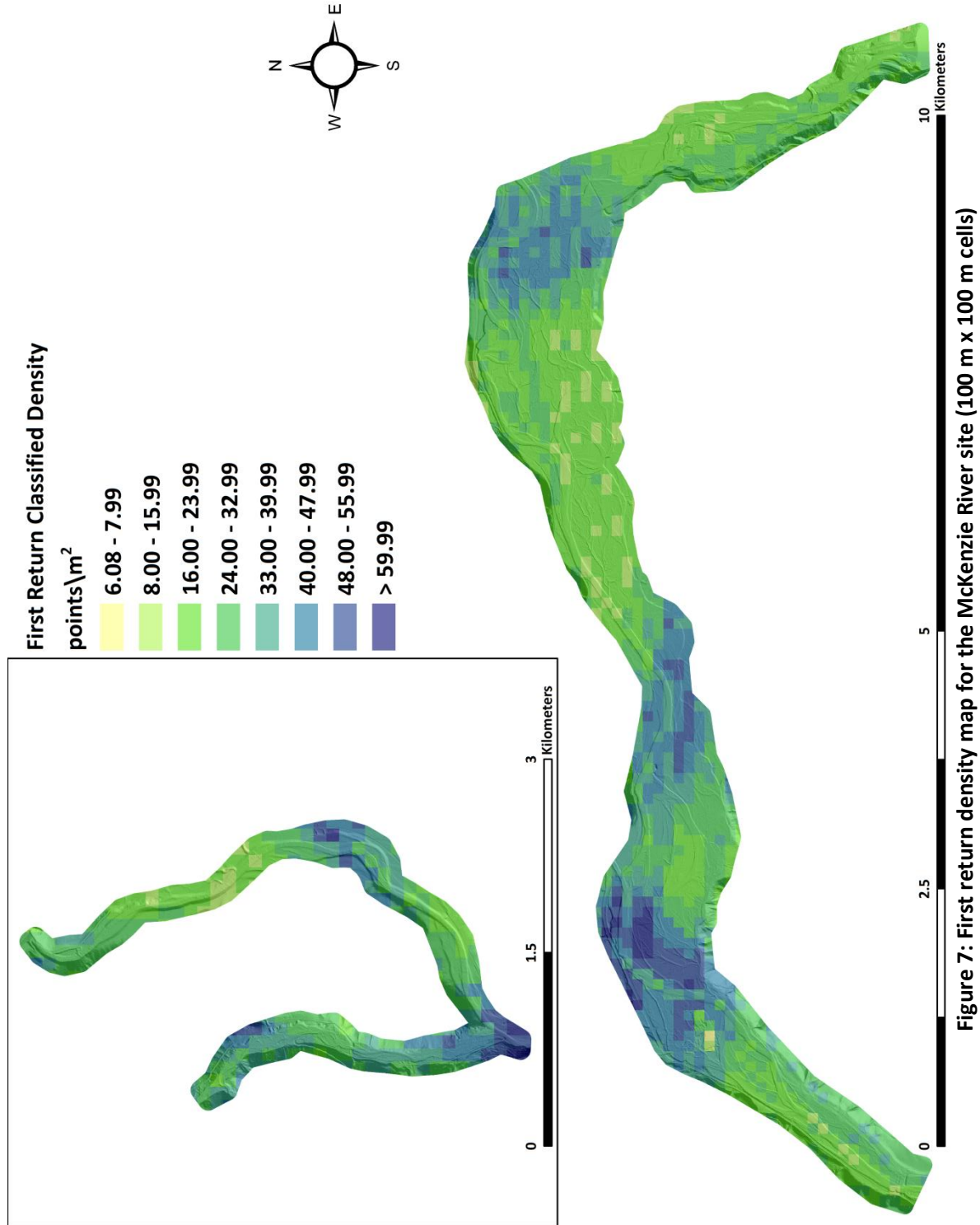
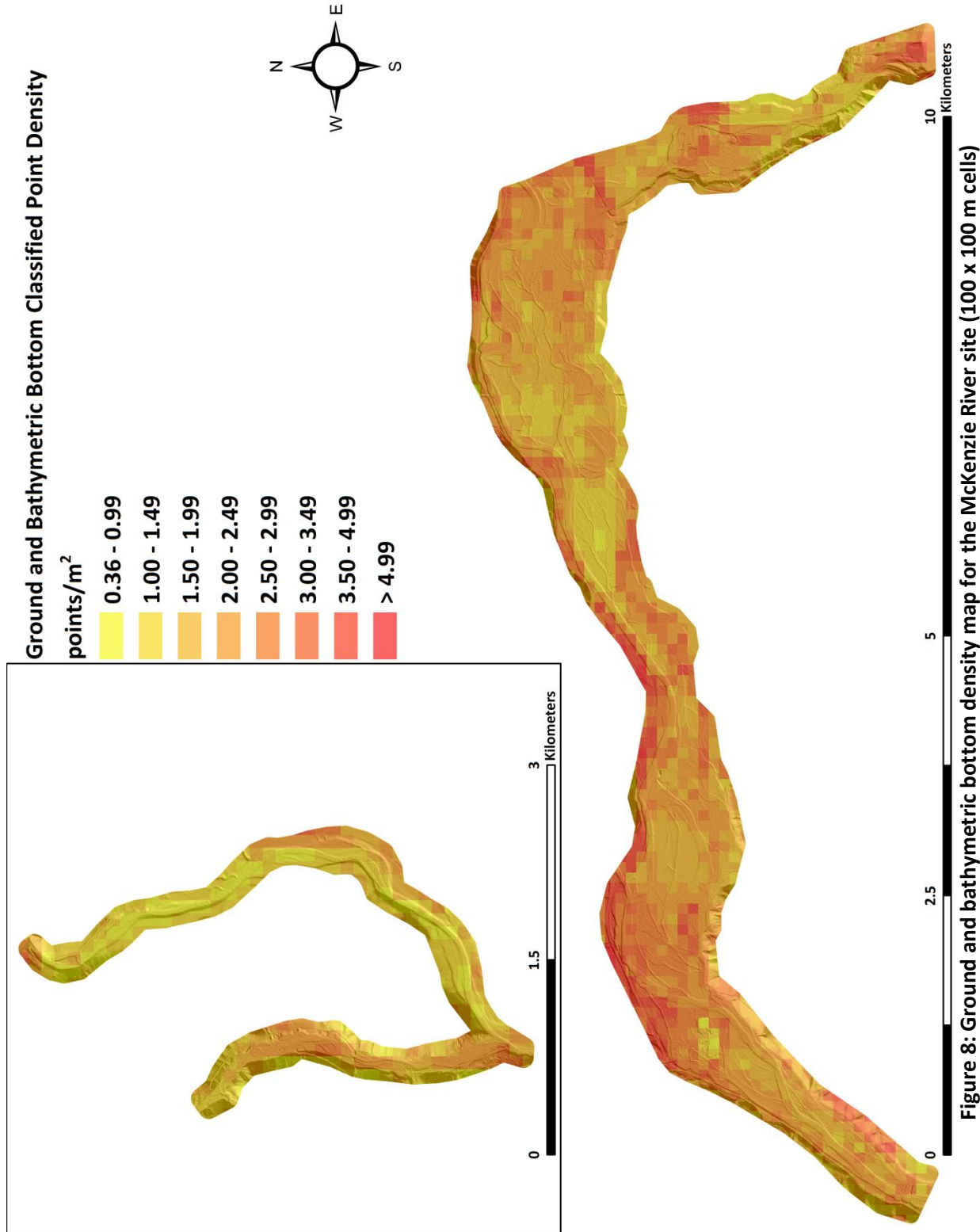


Figure 7: First return density map for the McKenzie River site (100 m x 100 m cells)



## LiDAR Accuracy Assessments

The accuracy of the LiDAR data collection can be described in terms of absolute accuracy (the consistency of the data with external data sources) and relative accuracy (the consistency of the dataset with itself). See Appendix A for further information on sources of error and operational measures used to improve relative accuracy.

### LiDAR Non-Vegetated Vertical Accuracy

Absolute accuracy was assessed using Non-vegetated Vertical Accuracy (NVA) reporting designed to meet guidelines presented in the FGDC National Standard for Spatial Data Accuracy<sup>1</sup>. NVA compares known ground quality assurance point data collected on open, bare earth surfaces with level slope (<20°) to the triangulated surface generated by the LiDAR points. NVA is a measure of the accuracy of LiDAR point data in open areas where the LiDAR system has a high probability of measuring the ground surface and is evaluated at the 95% confidence interval (1.96 \* RMSE), as shown in Table 10.

The mean and standard deviation (sigma  $\sigma$ ) of divergence of the ground surface model from ground check point coordinates are also considered during accuracy assessment. These statistics assume the error for x, y and z is normally distributed, and therefore the skew and kurtosis of distributions are also considered when evaluating error statistics. For the McKenzie River survey, 40 ground check points were withheld from the calibration and post-processing of the LiDAR point cloud, with resulting non-vegetated vertical accuracy of 0.062 meters as compared to the unclassified point cloud and 0.071 meters as compared to the bare earth DEM, with 95% confidence.

Submerged bathymetric check points were also collected in order to assess the submerged surface vertical accuracy. Assessment of 5 bathymetric check points resulted in an average vertical accuracy of 0.015 meters (Table 10, Figure 11).

QSI also assessed absolute accuracy using 112 ground control points. Although these points were used in the calibration and post-processing of the LiDAR point cloud, they still provide a good indication of the overall accuracy of the LiDAR dataset, and therefore have been provided in Table 10 and Figure 12.

---

<sup>1</sup> Federal Geographic Data Committee, ASPRS POSITIONAL ACCURACY STANDARDS FOR DIGITAL GEOSPATIAL DATA EDITION 1, Version 1.0, NOVEMBER 2014. <http://www.asprs.org/PAD-Division/ASPRS-POSITIONAL-ACCURACY-STANDARDS-FOR-DIGITAL-GEOSPATIAL-DATA.html>.

**Table 10: Absolute accuracy (NVA) results**

Non-Vegetated Vertical Accuracy				
	Ground Check Points (Unclassified LAS Point Cloud)	Ground Check Points (Bare Earth DEM)	Bathymetric Check Points	Ground Control Points
<b>Sample</b>	40 points	40 points	5 points	112 points
<b>95% Confidence (1.96*RMSE)</b>	0.062 m	0.071 m	N/A	0.058 m
<b>95<sup>th</sup> Percentile</b>	N/A	N/A	0.015 m	N/A
<b>Average</b>	0.020 m	-0.009 m	-0.001 m	-0.005 m
<b>Median</b>	0.022 m	0.001 m	-0.001 m	-0.002 m
<b>RMSE</b>	0.032 m	0.036 m	0.012 m	0.030 m
<b>Standard Deviation (1<math>\sigma</math>)</b>	0.025m	0.036 m	0.013 m	0.029 m

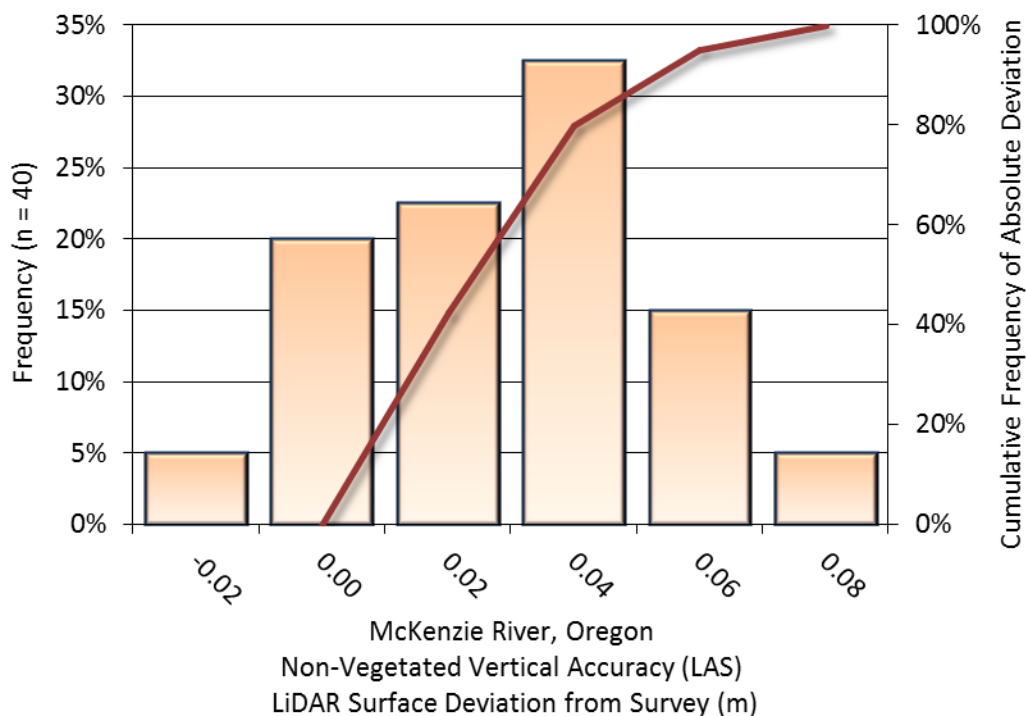


**Figure 9: Frequency histogram for LiDAR surface deviation from ground check point values as compared to the unclassified point cloud**

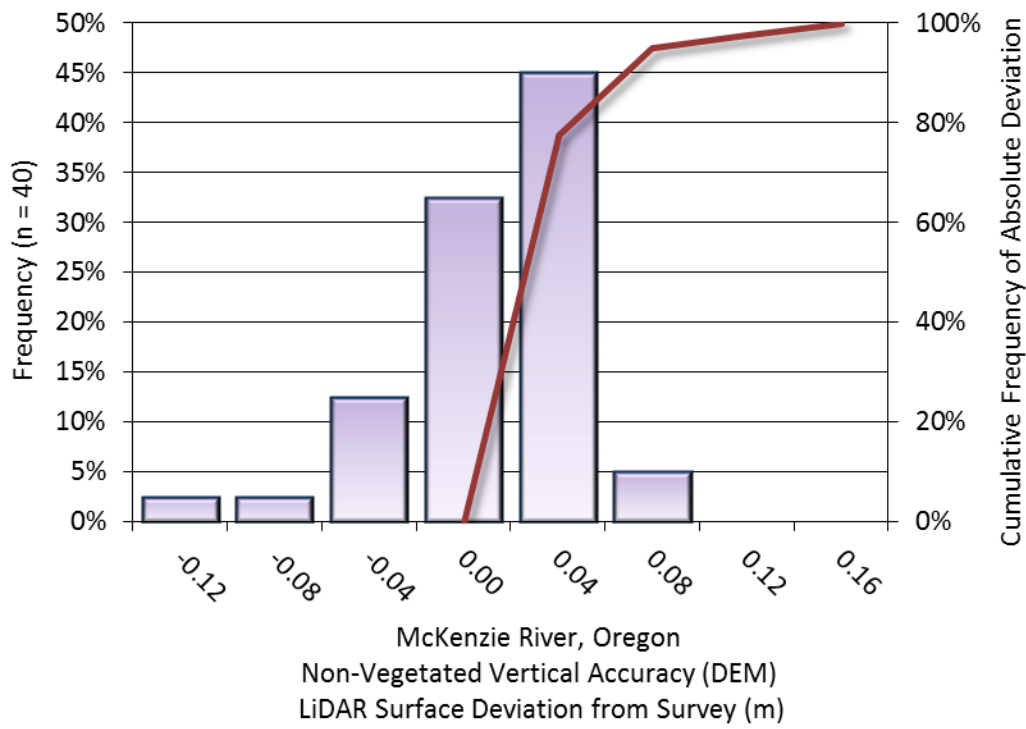


**Figure 10: Frequency histogram for LiDAR surface deviation from ground check point values as compared to the bare earth digital elevation model**

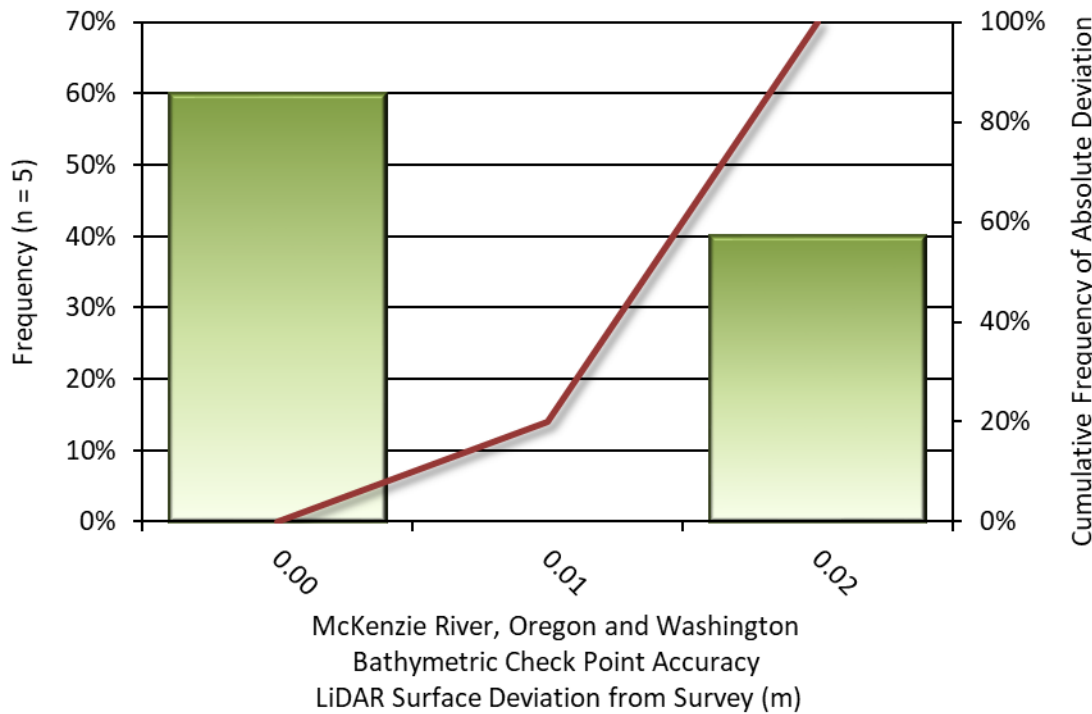


**Figure 11: Frequency histogram for LiDAR surface deviation from bathymetric check point values**

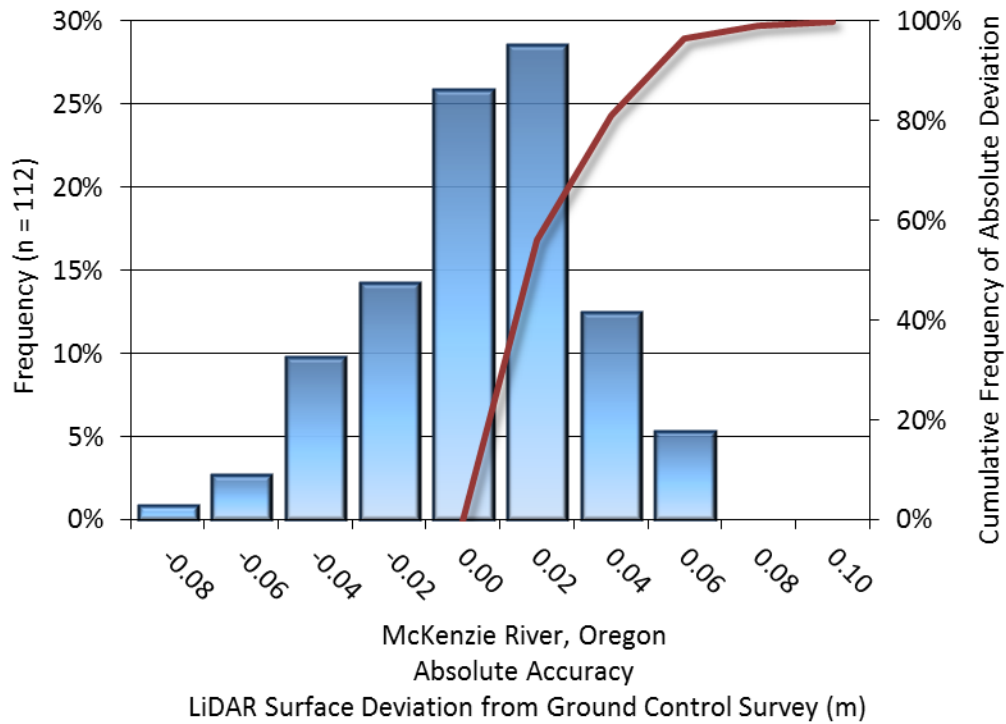


**Figure 12: Frequency histogram for LiDAR surface deviation from ground control point values**

## LiDAR Vegetated Vertical Accuracies

QSI also assessed vertical accuracy using Vegetated Vertical Accuracy (VVA) reporting. VVA compares known ground check point data collected over vegetated surfaces using land class descriptions to the triangulated ground surface generated by the ground classified LiDAR points. VVA is evaluated at the 95<sup>th</sup> percentile (Table 11, Figure 13).

**Table 11: Vegetated Vertical Accuracy for the McKenzie River Project**

Vegetated Vertical Accuracy (VVA)	
Sample	8 points
Average Dz	0.050 m
Median	0.064 m
RMSE	0.064 m
Standard Deviation (1 $\sigma$ )	0.044 m
95 <sup>th</sup> Percentile	0.089 m

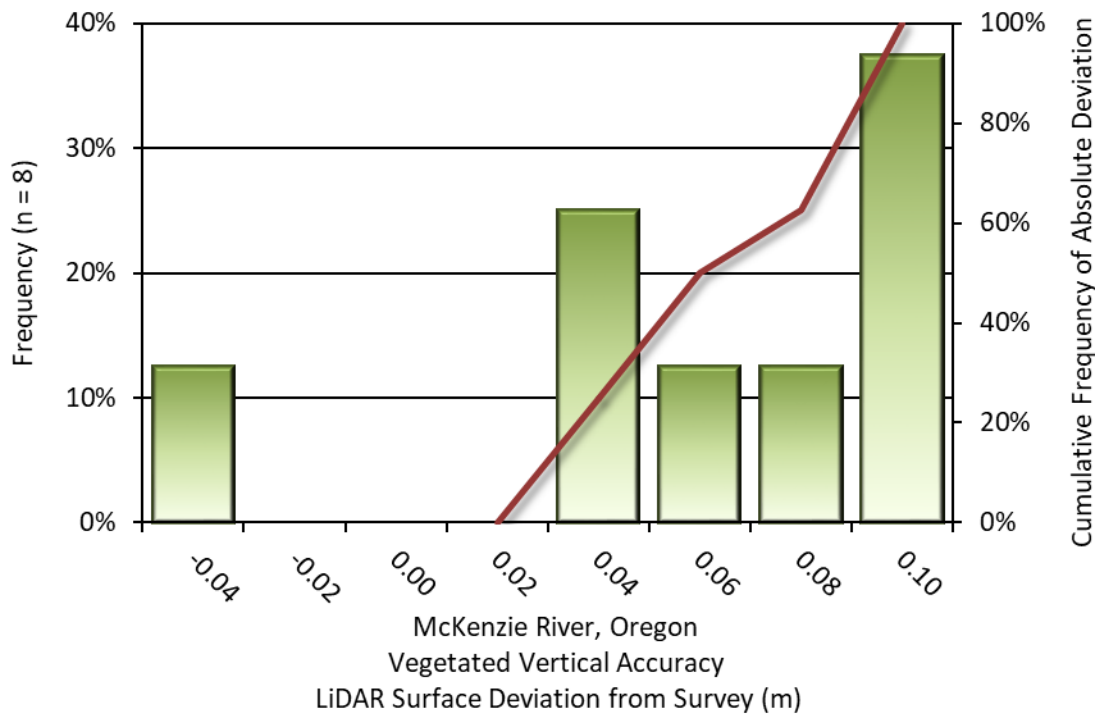


**Figure 13: Frequency histogram for LiDAR surface deviation from all land cover class point values (VVA)**

## LiDAR Relative Vertical Accuracy

Relative vertical accuracy refers to the internal consistency of the data set as a whole: the ability to place an object in the same location given multiple flight lines, GPS conditions, and aircraft attitudes. When the LiDAR system is well calibrated, the swath-to-swath vertical divergence is low (<0.10 meters). The relative vertical accuracy was computed by comparing the ground surface model of each individual flight line with its neighbors in overlapping regions. The average (mean) line to line relative vertical accuracy for the McKenzie River LiDAR project was 0.044 meters (Table 12, Figure 14).

**Table 12: Relative accuracy results**

Relative Accuracy	
<b>Sample</b>	114 surfaces
<b>Average</b>	0.044 m
<b>Median</b>	0.049 m
<b>RMSE</b>	0.051 m
<b>Standard Deviation (1<math>\sigma</math>)</b>	0.012 m
<b>1.96<math>\sigma</math></b>	0.024m

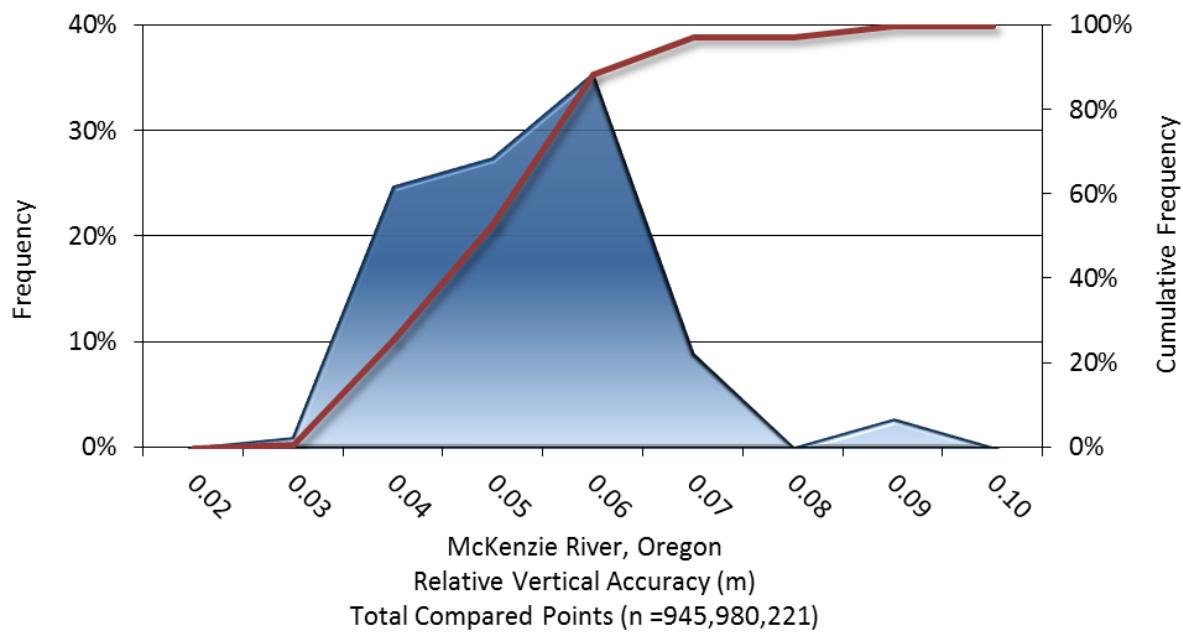


**Figure 14: Frequency plot for relative vertical accuracy between flight lines**

## CERTIFICATIONS

Quantum Spatial, Inc. provided LiDAR services for the McKenzie River project as described in this report.

I, Tucker Selko, have reviewed the attached report for completeness and hereby state that it is a complete and accurate report of this project.

Tucker Selko  
Tucker Selko (Jul 20, 2018)

Jul 20, 2018

Tucker Selko  
Project Manager  
Quantum Spatial, Inc.

I, Evon P. Silvia, PLS, being duly registered as a Professional Land Surveyor in and by the state of Oregon, hereby certify that the methodologies, static GNSS occupations used during airborne flights, and ground survey point collection were performed using commonly accepted Standard Practices. Field work conducted for this report was conducted between April 26 and 29, 2018.

Accuracy statistics shown in the Accuracy Section of this Report have been reviewed by me and found to meet the "National Standard for Spatial Data Accuracy".

Evon P. Silvia Jul 20, 2018

Evon P. Silvia, PLS  
Quantum Spatial, Inc.  
Corvallis, OR 97330

REGISTERED  
PROFESSIONAL  
LAND SURVEYOR

Evon P. Silvia

OREGON  
JUNE 10, 2014  
EVON P. SILVIA  
81104LS

EXPIRES: 06/30/2020

## SELECTED IMAGES

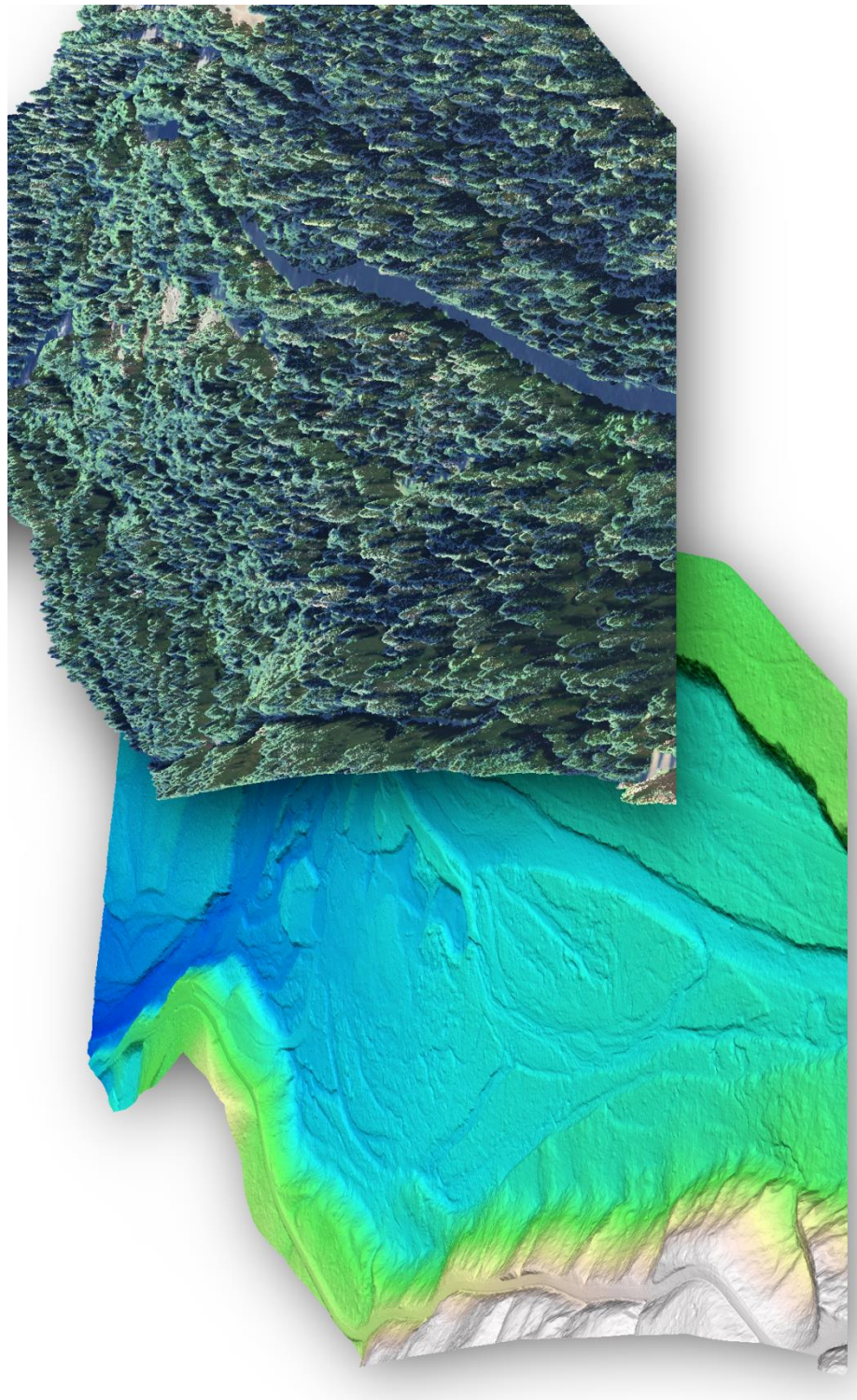


**Figure 15:** View looking northwest over McKenzie River. The top image was created from the LiDAR bare earth model overlaid with the above ground point cloud and colored by NAIP imagery. The bottom image was created from the LiDAR bare earth model and colored by elevation.

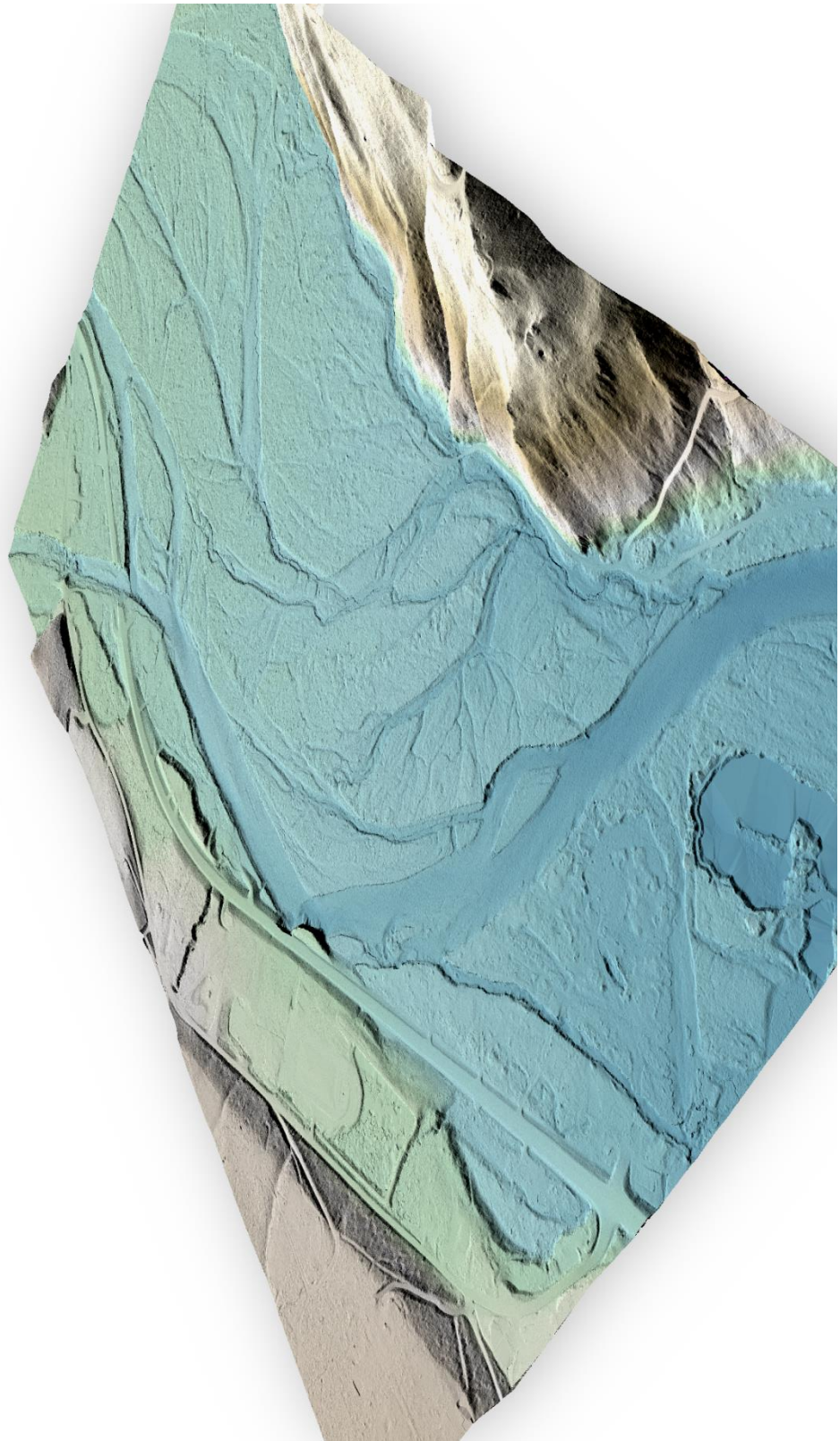


Figure 16: View looking northeast over McKenzie River. The image was created from the LiDAR bare earth model colored by elevation.

## GLOSSARY

**1-sigma ( $\sigma$ ) Absolute Deviation:** Value for which the data are within one standard deviation (approximately 68<sup>th</sup> percentile) of a normally distributed data set.

**1.96 \* RMSE Absolute Deviation:** Value for which the data are within two standard deviations (approximately 95<sup>th</sup> percentile) of a normally distributed data set, based on the FGDC standards for Non-vegetated Vertical Accuracy (FVA) reporting.

**Accuracy:** The statistical comparison between known (surveyed) points and laser points. Typically measured as the standard deviation (sigma  $\sigma$ ) and root mean square error (RMSE).

**Absolute Accuracy:** The vertical accuracy of LiDAR data is described as the mean and standard deviation (sigma  $\sigma$ ) of divergence of LiDAR point coordinates from ground survey point coordinates. To provide a sense of the model predictive power of the dataset, the root mean square error (RMSE) for vertical accuracy is also provided. These statistics assume the error distributions for x, y and z are normally distributed, and thus we also consider the skew and kurtosis of distributions when evaluating error statistics.

**Relative Accuracy:** Relative accuracy refers to the internal consistency of the data set; i.e., the ability to place a laser point in the same location over multiple flight lines, GPS conditions and aircraft attitudes. Affected by system attitude offsets, scale and GPS/IMU drift, internal consistency is measured as the divergence between points from different flight lines within an overlapping area. Divergence is most apparent when flight lines are opposing. When the LiDAR system is well calibrated, the line-to-line divergence is low (<10 cm).

**Root Mean Square Error (RMSE):** A statistic used to approximate the difference between real-world points and the LiDAR points. It is calculated by squaring all the values, then taking the average of the squares and taking the square root of the average.

**Data Density:** A common measure of LiDAR resolution, measured as points per square meter.

**Digital Elevation Model (DEM):** File or database made from surveyed points, containing elevation points over a contiguous area. Digital terrain models (DTM) and digital surface models (DSM) are types of DEMs. DTMs consist solely of the bare earth surface (ground points), while DSMs include information about all surfaces, including vegetation and man-made structures.

**Intensity Values:** The peak power ratio of the laser return to the emitted laser, calculated as a function of surface reflectivity.

**Nadir:** A single point or locus of points on the surface of the earth directly below a sensor as it progresses along its flight line.

**Overlap:** The area shared between flight lines, typically measured in percent. 100% overlap is essential to ensure complete coverage and reduce laser shadows.

**Pulse Rate (PR):** The rate at which laser pulses are emitted from the sensor; typically measured in thousands of pulses per second (kHz).

**Pulse Returns:** For every laser pulse emitted, the number of wave forms (i.e., echoes) reflected back to the sensor. Portions of the wave form that return first are the highest element in multi-tiered surfaces such as vegetation. Portions of the wave form that return last are the lowest element in multi-tiered surfaces.

**Real-Time Kinematic (RTK) Survey:** A type of surveying conducted with a GPS base station deployed over a known monument with a radio connection to a GPS rover. Both the base station and rover receive differential GPS data and the baseline correction is solved between the two. This type of ground survey is accurate to 1.5 cm or less.

**Post-Processed Kinematic (PPK) Survey:** GPS surveying is conducted with a GPS rover collecting concurrently with a GPS base station set up over a known monument. Differential corrections and precisions for the GNSS baselines are computed and applied after the fact during processing. This type of ground survey is accurate to 1.5 cm or less.

**Scan Angle:** The angle from nadir to the edge of the scan, measured in degrees. Laser point accuracy typically decreases as scan angles increase.

**Native LiDAR Density:** The number of pulses emitted by the LiDAR system, commonly expressed as pulses per square meter.

## APPENDIX A - ACCURACY CONTROLS

### Relative Accuracy Calibration Methodology:

Manual System Calibration: Calibration procedures for each mission require solving geometric relationships that relate measured swath-to-swath deviations to misalignments of system attitude parameters. Corrected scale, pitch, roll and heading offsets were calculated and applied to resolve misalignments. The raw divergence between lines was computed after the manual calibration was completed and reported for each survey area.

Automated Attitude Calibration: All data were tested and calibrated using TerraMatch automated sampling routines. Ground points were classified for each individual flight line and used for line-to-line testing. System misalignment offsets (pitch, roll and heading) and scale were solved for each individual mission and applied to respective mission datasets. The data from each mission were then blended when imported together to form the entire area of interest.

Automated Z Calibration: Ground points per line were used to calculate the vertical divergence between lines caused by vertical GPS drift. Automated Z calibration was the final step employed for relative accuracy calibration.

### LiDAR accuracy error sources and solutions:

Type of Error	Source	Post Processing Solution
<b>GPS</b> <b>(Static/Kinematic)</b>	Long Base Lines	None
	Poor Satellite Constellation	None
	Poor Antenna Visibility	Reduce Visibility Mask
<b>Relative Accuracy</b>	Poor System Calibration	Recalibrate IMU and sensor offsets/settings
	Inaccurate System	None
<b>Laser Noise</b>	Poor Laser Timing	None
	Poor Laser Reception	None
	Poor Laser Power	None
	Irregular Laser Shape	None

### Operational measures taken to improve relative accuracy:

Low Flight Altitude: Terrain following was employed to maintain a constant above ground level (AGL). Laser horizontal errors are a function of flight altitude above ground (about 1/3000<sup>th</sup> AGL flight altitude).

Focus Laser Power at narrow beam footprint: A laser return must be received by the system above a power threshold to accurately record a measurement. The strength of the laser return (i.e., intensity) is a function of laser emission power, laser footprint, flight altitude and the reflectivity of the target. While surface reflectivity cannot be controlled, laser power can be increased and low flight altitudes can be maintained.

Reduced Scan Angle: Edge-of-scan data can become inaccurate. The scan angle was reduced to a maximum of  $\pm 20^\circ$  from nadir, creating a narrow swath width and greatly reducing laser shadows from trees and buildings.

Quality GPS: Flights took place during optimal GPS conditions (e.g., 6 or more satellites and PDOP [Position Dilution of Precision] less than 3.0). Before each flight, the PDOP was determined for the survey day. During all flight times, a dual frequency DGPS base station recording at 1 second epochs was utilized and a maximum baseline length between the aircraft and the control points was less than 13 nm at all times.

Ground Survey: Ground survey point accuracy (<1.5 cm RMSE) occurs during optimal PDOP ranges and targets a minimal baseline distance of 4 miles between GPS rover and base. Robust statistics are, in part, a function of sample size (n) and distribution. Ground survey points are distributed to the extent possible throughout multiple flight lines and across the survey area.

50% Side-Lap (100% Overlap): Overlapping areas are optimized for relative accuracy testing. Laser shadowing is minimized to help increase target acquisition from multiple scan angles. Ideally, with a 50% side-lap, the nadir portion of one flight line coincides with the swath edge portion of overlapping flight lines. A minimum of 50% side-lap with terrain-followed acquisition prevents data gaps.

Opposing Flight Lines: All overlapping flight lines have opposing directions. Pitch, roll and heading errors are amplified by a factor of two relative to the adjacent flight line(s), making misalignments easier to detect and resolve.